

Reactions of 2-indolylphosphines with $\text{Ru}_3(\text{CO})_{12}$: cluster capping with μ_3, η^2 -indolylphosphine as an anionic six-electron P,N-donor ligand

Edmond Lam, David H. Farrar,* C. Scott Browning and Alan J. Lough

Davenport Chemical Research Building, University of Toronto, 80 St. George Street, Toronto, Ontario, Canada, M5S 3H6. E-mail: dfarrar@chem.utoronto.ca; Fax: (+416) 946-7526; Tel: (+416) 946-7526

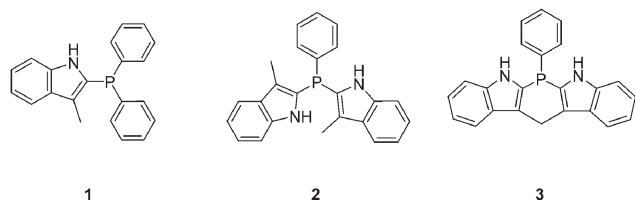
Received 30th June 2004, Accepted 16th August 2004

First published as an Advance Article on the web 9th September 2004

Stepwise bidentate coordination of the novel indolylphosphine ligands HL (**1**, HL = $\text{P}(\text{C}_6\text{H}_5)_2(\text{C}_9\text{H}_8\text{N})$ (diphenyl-2-(3-methylindolyl)phosphine); **2**, HL = $\text{P}(\text{C}_6\text{H}_5)(\text{C}_9\text{H}_8\text{N})_2$ (phenyldi-2-(3-methylindolyl)phosphine); and **3**, HL = $\text{P}(\text{C}_6\text{H}_5)(\text{C}_{17}\text{H}_{12}\text{N}_2)$ (di(1*H*-3-indolyl)methane-(2,12)-phenylphosphine)) to the ruthenium cluster $\text{Ru}_3(\text{CO})_{12}$ is demonstrated. Reactions of **1–3** with $\text{Ru}_3(\text{CO})_{12}$ led to the formation of $\text{Ru}_3(\text{CO})_{11}(\text{HL})$ (**4–6**), in which HL is mono-coordinated through the phosphorus atom. The X-ray structures of **4–6** show that the phosphorus atom is equatorially coordinated to the triruthenium core. In all cases, gentle heating of $\text{Ru}_3(\text{CO})_{11}(\text{HL})$ resulted in the formation of $\text{Ru}_3(\text{CO})_9(\mu\text{-H})(\mu_3, \eta^2\text{-L})$ (**7–9**) in which the NH proton of the indolyl substituent had migrated to the ruthenium core to form a bridging hydride ligand. The X-ray structure of $\text{Ru}_3(\text{CO})_9(\mu\text{-H})[\mu_3, \eta^2\text{-P}(\text{C}_6\text{H}_5)_2(\text{C}_9\text{H}_7\text{N})]$ (**7**) shows the deprotonated nitrogen atom of the indolyl moiety bridging over the face of the triruthenium core, bonding to the two ruthenium metal centers to which the phosphorus atom is not bound. The phosphorus atom is forced to adopt an axial bonding mode due to the geometry of the indolylphosphine ligand. Cluster electron counting and X-ray data suggest that the indolylphosphine behaves as a six-electron ligand in this mode of coordination. Compounds **4–9** have been characterized by IR, ^1H , ^{13}C and ^{31}P NMR spectroscopy.

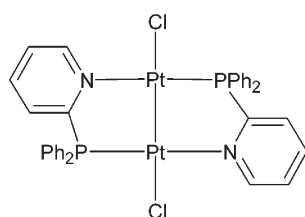
Introduction

We have recently reported the synthesis of several new indolylphosphine ligands HL (**1**, HL = $\text{P}(\text{C}_6\text{H}_5)_2(\text{C}_9\text{H}_8\text{N})$ (diphenyl-3-methylindolylphosphine); **2**, HL = $\text{P}(\text{C}_6\text{H}_5)(\text{C}_9\text{H}_8\text{N})_2$ (phenyldi(3-methylindolyl)phosphine); and **3**, HL = $\text{P}(\text{C}_6\text{H}_5)(\text{C}_{17}\text{H}_{12}\text{N}_2)$ (di(1*H*-3-indolyl)methane-(2,12)-phenylphosphine)) in which the phosphorus atom is bound to the C2 position of the indolyl substituent.¹



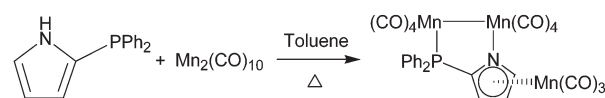
The synthesis of these ligands was carried out by using a (dialkylamino)methyl protecting group to direct lithiation at the C2 position of the indole,² followed by electrophilic substitution of a phosphonous acid dichloride (RPCl_2) or phosphinous acid chloride (R_2PCl) to give the desired ligand. In the absence of base with which to deprotonate NH, the coordination of these ligands to palladium occurred exclusively at the phosphorus atom.¹

These 2-indolylphosphines bear closest resemblance to diphenyl(2-pyrrolyl)phosphine and the 2-pyridinylphosphines. There are many examples in the chemical literature of P–C–N bridges across two metal centers using the latter ligands,³ as observed in the complex $\text{Pt}_2\text{Cl}_2(\text{PPh}_2\text{Py})_2$ ^{3a} (where Py =



2-pyridinyl). In these ligands, both the nitrogen and phosphorus centers serve as two-electron donors.

The 2-indolylphosphines^{1,4} notwithstanding, diphenyl(2-pyrrolyl)phosphine, $\text{PPh}_2(2\text{-C}_4\text{H}_3\text{NH})$, is the only P-donor ligand that features a protic hydrogen on an aromatic substituent. In addition to its difficult synthesis, its unpredictable coordination chemistry has hindered investigations into the behavior of $\text{PPh}_2(2\text{-C}_4\text{H}_3\text{NH})$ as a ligand. Its reaction with $\text{Mn}_2(\text{CO})_{10}$ to obtain the complex $\text{Mn}_3(\mu_3\text{-P}, \text{N}-\eta^5\text{-Ph}_2\text{PC}_4\text{H}_3\text{N})(\text{CO})_{11}$ (Scheme 1) in low yield as one of three products⁵ represents the only example of an anionic nitrogen centre in a phosphine ligand. In addition to η^5 -coordination of the azacyclopentadienyl ring to a manganese tricarbonyl unit, deprotonation of the nitrogen atom occurs, allowing the diphenyl-2-pyrrolylphosphine ligand to bridge across the $\text{Mn}_2(\text{CO})_8$ unit as a four-electron donor.



Scheme 1

As part of an ongoing examination into the behaviour of the 2-indolylphosphines, we herein report the investigation of the additional reactivity of the NH moiety of the indolyl substituents of the coordinated ligands **1–3**. The metal carbonyl cluster $\text{Ru}_3(\text{CO})_{12}$ was chosen as the platform for this study because of previous studies in the literature in which the reactions of $\text{Ru}_3(\text{CO})_{12}$ with closely related ligands such as PPh_2Py are well characterized. The substitution reactions of monodentate tertiary phosphine ligands⁶ to yield $\text{Ru}_3(\text{CO})_{11}\text{L}$ occurs favourably *via* a radical reaction using sodium diphenylketyl as the initiator.^{6a}

The Ph_2CO^- catalyzed reactions between $\text{Ru}_3(\text{CO})_{12}$ and the indolylphosphine ligands **1–3** give the mono-substituted clusters $\text{Ru}_3(\text{CO})_{11}(\text{HL})$ (**4–6**) in which coordination of the ligand occurs only at the phosphorus atom. These reactions give very high yields. We then demonstrate the ability of the indolylphosphine ligand to bridge metal centers in the synthesis

Table 1 Crystallographic and refinement data for clusters **4**, **5**, **6** and **7**-C₆D₆

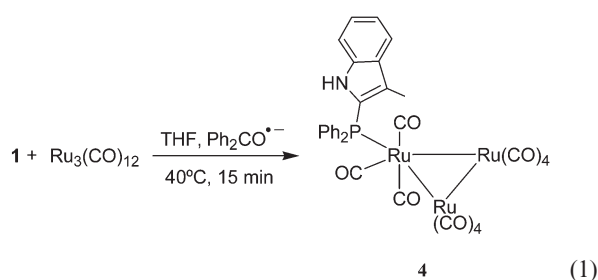
	4	5	6	7
Empirical formula	C ₃₂ H ₁₈ NO ₁₁ PRu ₃	C ₃₅ H ₂₁ N ₂ O ₁₁ PRu ₃	C ₃₄ H ₁₇ N ₂ O ₁₁ PRu ₃	C ₃₆ H ₁₈ D ₆ NO ₉ PRu ₃
<i>M</i>	926.65	979.72	963.68	948.74
Crystal colour, shape	Red plate	Red plate	Red needle	Red needle
Crystal size/mm	0.14 × 0.12 × 0.08	0.13 × 0.10 × 0.10	0.20 × 0.10 × 0.10	0.12 × 0.12 × 0.10
Crystal system	Triclinic	Triclinic	Monoclinic	Triclinic
Space group	<i>P</i> $\bar{1}$	<i>P</i> $\bar{1}$	<i>P</i> 2 ₁ / <i>n</i>	<i>P</i> $\bar{1}$
<i>a</i> /Å	9.9970(2)	8.4910(2)	9.2360(3)	10.4643(3)
<i>b</i> /Å	11.4500(2)	12.7190(3)	35.246(1)	10.9306(3)
<i>c</i> /Å	14.8620(4)	16.6940(3)	10.4650(4)	15.8905(5)
<i>a</i> /°	100.723(1)	88.873(1)	90	106.70(1)
<i>β</i> /°	95.278(1)	78.824(1)	95.060(2)	94.64(1)
<i>γ</i> /°	100.585(1)	88.770(1)	90	91.27(1)
<i>V</i> /Å ³	1628.96(6)	1768.08(7)	3393.4(2)	1733.26(9)
<i>Z</i>	2	2	4	2
<i>D</i> _c /g cm ⁻³	1.889	1.84	1.886	1.818
<i>F</i> (000)	904	960	1880	932
<i>μ</i> (Mo-Kα)/cm ⁻¹	1.484	1.373	1.43	1.393
Limiting indices, <i>hkl</i>	-12 to 12 -14 to 14 -17 to 19	-10 to 11 -16 to 16 -20 to 21	-11 to 11 -45 to 45 -11 to 13	0 to 13 -14 to 14 -20 to 20
<i>θ</i> Range/°	2.67–27.47	2.90–27.51	2.61–27.50	2.67–27.34
Max. and min. transmission	0.892, 0.699	0.885, 0.510	0.868, 0.783	0.8733, 0.8507
No. of reflections collected	18107	19589	17172	13967
No. of independent reflections/ <i>R</i> _{int}	7390/435	8047/0.0554	7717/0.0438	7390/0.161
Extinction coefficient	0.0008(2)	0.0009(3)	none	0.0065(7)
No. of refined parameters	435	472	460	457
Final <i>R</i> ₁ , <i>wR</i> ₂	0.0362, 0.0788	0.0371, 0.0850	0.0411, 0.0785	0.0481, 0.1230
Final <i>R</i> ₁ , <i>wR</i> ₂ (all data)	0.0549, 0.0880	0.0526, 0.0938	0.0783, 0.0923	0.0757, 0.1442
Goodness of Fit	1.058	1.041	1.039	1.047
<i>Δρ</i> _{min,max} /e Å ⁻³	-0.989, 1.576	-1.327, 1.400	-0.822, 0.732	-1.434, 1.947

of Ru₃(CO)₉(μ-H)(μ₃,η²-L) (**7–9**). The resulting negatively charged nitrogen atom of the indolyl group axially bonds to two ruthenium atoms as a four-electron donor. We have been able to isolate the mono-substituted indolyl clusters Ru₃(CO)₁₁(HL) in good quantities without ligand fragmentation and subsequently effect their conversion to Ru₃(CO)₉(μ-H)(μ₃,η²-L) in a controlled, stepwise manner. A discussion of the bonding mode of the novel six-electron indolylphosphine ligand is described in the crystal structure of Ru₃(CO)₉(μ-H)[(μ₃,η²-P(C₆H₅)₂(C₉H₇N))] (**7**). The compounds **4–9** have been characterized by IR, ¹H, ¹³C and ³¹P NMR spectroscopy.

Results and discussion

Synthesis and characterization of Ru₃(CO)₁₁(HL) (**4–6**)

The 48-electron, red and air-stable mono-substituted cluster **4** was efficiently prepared by addition of a catalytic amount of Ph₂CO⁻ into a 1 : 1 orange coloured solution of Ru₃(CO)₁₂ and **1** in THF at 40 °C (eqn. (1)).



The reaction was complete within 5 min. The *ν*_{CO} absorption pattern of **4** was consistent with that of other previously characterized mono-substituted tertiary phosphine ruthenium clusters such as Ru₃(CO)₁₁(PPh₃).^{6a} Coordination of the indolylphosphine to the ruthenium cluster resulted in a downfield shift in the ³¹P NMR spectrum from *δ* -33.1 ppm for the free ligand **1** to *δ* 15.9 ppm for the cluster. The absence of any metal-hydride resonances in the ¹H NMR and a signal at *δ* 8.83 ppm for the NH proton confirmed that the nitrogen atom on the indole remained

protonated. The broadness of the single peak at *δ* 204.2 ppm in the ¹³C NMR suggested that the carbonyl ligands of the ruthenium cluster are fluxional in solution.

X-Ray quality crystals of **4** were grown from a saturated hexanes solution of the cluster. An ORTEP representation is given in Fig. 1. Crystallographic data for the crystal **4** is provided in Table 1. A selection of bond distances and angles is given in Table 2.

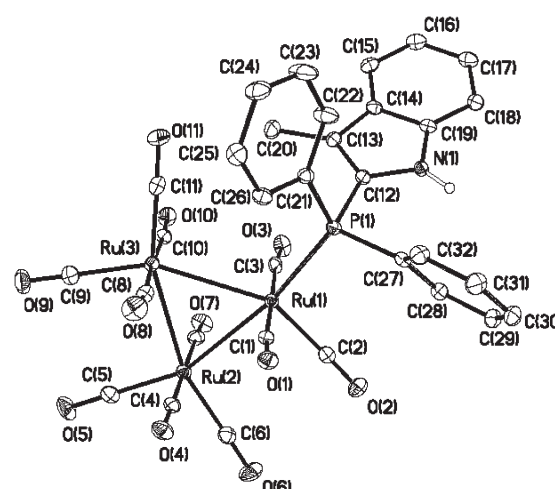


Fig. 1 ORTEP drawing of Ru₃(CO)₁₁[(P(C₆H₅)₂(C₉H₇N))] **4** with atoms shown as 30% probability ellipsoids. Phenyl hydrogen atoms have been omitted for clarity.

The crystal structure confirms substitution of a carbonyl group by the indolylphosphine **1** in the triruthenium core. P(1) is bonded equatorially to the Ru(1) atom with a bond length of 2.3665(9) Å. The Ru(1)–P(1) bond length is comparable to the Ru–P bond length of 2.380(6) Å for Ru₃(CO)₁₁(PPh₃) in which the phosphorus atom is similarly bonded equatorially to the ruthenium cluster.⁷ Eleven carbonyl ligands complete the ligand shell of the cluster. The NH proton was found in the difference

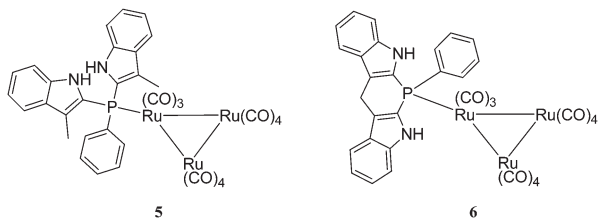
Table 2 Selected bond distances (Å) and bond angles (°) for clusters 4–6

	4	5	6
Ru(1)–Ru(2)	2.8628(7)	2.8449(4)	2.8604(5)
Ru(1)–Ru(3)	2.9014(7)	2.8693(7)	2.8894(5)
Ru(2)–Ru(3)	2.8648(7)	2.8411(7)	2.8641(5)
Ru(3)–P(1)	2.3665(9)	2.3597(9)	2.343(1)
N(1)–C(12)	1.389(4)	1.389(4)	1.394(4)
N(1)–C(19)	1.380(4)	1.381(4)	1.381(5)
P(1)–C(12)	1.818(4)	1.809(3)	1.800(4)
C(12)–C(13)	1.372(5)	1.376(5)	1.367(5)
C(13)–C(14)	1.426(5)	1.448(5)	1.429(5)
C(14)–C(19)	1.417(5)	1.402(5)	1.407(5)
Ru(1)–Ru(2)–Ru(3)	60.87(1)	60.612(9)	60.63(1)
Ru(1)–Ru(3)–Ru(2)	59.532(9)	59.760(9)	59.62(1)
Ru(2)–Ru(1)–Ru(3)	59.60(1)	59.628(9)	59.75(1)
Ru(1)–P(1)–C(12)	117.7(1)	113.5(1)	111.5(1)
P(1)–C(12)–N(1)	122.6(2)	119.6(3)	121.8(3)
C(12)–N(1)–C(19)	109.4(3)	103.3(4)	108.4(3)
C(12)–C(13)–C(14)	107.2(3)	106.5(3)	107.2(3)
C(13)–C(14)–C(19)	107.6(3)	107.3(3)	107.3(3)
C(14)–C(19)–N(1)	106.8(3)	107.7(3)	107.8(3)

Fourier map confirming that the indole nitrogen atom of the ligand remains protonated.

In adopting a terminal, equatorial mode of coordination in **4**, **1** serves as a classic monodentate P-donor ligand. This behaviour lies in contrast to the reactivity observed for $\text{PPh}_2(2\text{-C}_6\text{H}_3\text{NH})$ and PPh_2Py toward $\text{Ru}_3(\text{CO})_{12}$.^{8,9} In both cases, the mono-substituted $\text{Ru}_3(\text{CO})_{11}\text{L}$ clusters were not isolated in good yields as they undergo further reaction under ambient conditions (*vide infra*).

The analogous clusters **5** and **6** were prepared in similar fashion and exhibit comparable ν_{CO} IR absorption patterns to **4**.



Ligands **2** and **3** also exhibited similar downfield changes in their ^{31}P NMR chemical shifts as **1** upon bonding to the triruthenium core. The absence of any metal–hydride resonances in the ^1H NMR spectrum suggested that the NH proton had not been transferred to the cluster. X-Ray quality crystals of **5** and **6** were also grown from saturated hexanes solutions of the clusters to confirm the structure of both. ORTEP representations of **5** and **6** are shown in Figs. 2 and 3, respectively.

Crystallographic data for the crystals of **5** and **6** are given in Table 1. A selection of bond distances and angles for both crystals is presented in Table 2. Similarly to **4**, electron difference maps demonstrate that the indole nitrogens in **5** and **6** remain protonated. In **5** and **6**, P(1) is bonded equatorially to Ru(1). Intermolecular hydrogen bonding exists in **5** between N(1)–H(1A) of one cluster and carbonyl O(6) of its crystallographic partner in the unit cell. Two sets of hydrogen bonding interactions are present in the crystal lattice of **6**. N(1)–H(1A) hydrogen bonds intramolecularly with carbonyl O(1) while N(2)–H(2A) hydrogen bonds intermolecularly with carbonyl O(6) as observed in **5**. Hydrogen bonding between NH of the phosphine and chloride ligands of palladium was previously reported in the crystal structures of $\text{Pd}_2\text{Cl}_4[\text{P}(\text{C}_6\text{H}_5)_2(\text{C}_9\text{H}_8\text{N})]_2$, $\text{Pd}_2\text{Cl}_4[\text{P}(\text{C}_6\text{H}_5)(\text{C}_9\text{H}_8\text{N})]_2$ and $\text{Pd}_2\text{Cl}_4[\text{P}(\text{C}_6\text{H}_5)(\text{C}_{17}\text{H}_{12}\text{N}_2)]_2$.¹ As with **1**, the ligands **2** and **3** serve as classic monodentate two-electron P-donors upon substitution of $\text{Ru}_3(\text{CO})_{12}$.

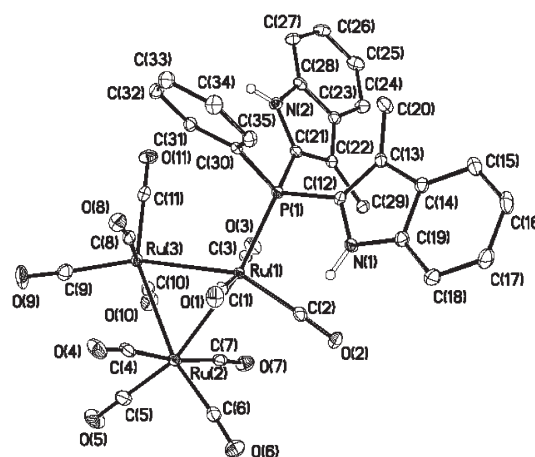


Fig. 2 ORTEP drawing of $\text{Ru}_3(\text{CO})_{11}[\text{P}(\text{C}_6\text{H}_5)(\text{C}_9\text{H}_8\text{N})]_2$ **5** with atoms shown as 30% probability ellipsoids. Phenyl hydrogen atoms have been omitted for clarity.

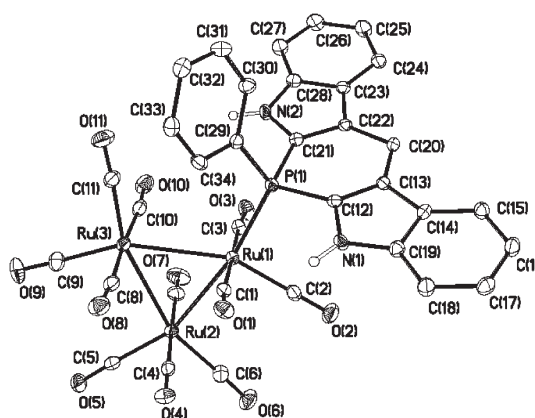
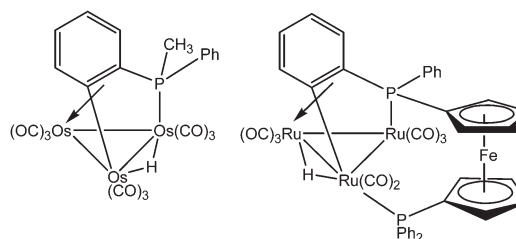


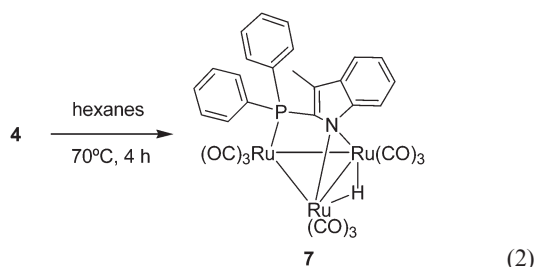
Fig. 3 ORTEP drawing of $\text{Ru}_3(\text{CO})_{11}[\text{P}(\text{C}_6\text{H}_5)(\text{C}_{17}\text{H}_{12}\text{N}_2)]_2$ **6** with atoms shown as 30% probability ellipsoids. Phenyl hydrogen atoms have been omitted for clarity.

Synthesis and characterization of $\text{Ru}_3(\text{CO})_9(\mu\text{-H})(\mu_3, \eta^2\text{-L})$ (**7–9**)

The extensive H-bonding involving the indole substituents of ligands **1–3** in their palladium complexes¹ corroborated our belief that the NH group would serve as an additional site of reactivity in these ligands. Metallation of coordinated phosphines in trinuclear clusters of Group 8 metals has occurred previously at elevated temperatures.^{10,11} Decarbonylation of $\text{Os}_3(\text{CO})_{11}(\text{PPh}_2\text{Me})$ in refluxing octane led to the formation of six products, one of which was $\text{Os}_3\text{H}(\text{C}_6\text{H}_4\text{PMePh})(\text{CO})_9$ where the μ_3 -phosphine is bound through phosphorus at one osmium center and through the metallated phenyl ring to the remaining two osmium centers.¹⁰ Similarly, pyrolysis of $\text{Ru}_3(\text{CO})_{10}(\text{diphenylphosphinoferrrocene})$ afforded $\text{Ru}_3(\mu\text{-H})\{\mu_3\text{-PPh}(\eta^1, \eta^2\text{-C}_6\text{H}_4)(\eta\text{-C}_5\text{H}_4)\text{-Fe}(\eta\text{-C}_5\text{H}_4\text{PPh}_2)\}(\text{CO})_8$ in low yield as one of eighteen products.¹¹



The gentle heating of cluster **4** in hexanes at 70 °C (eq. 2) was monitored by IR spectroscopy. The characteristic ν_{CO} IR absorption of **4** disappeared, leading to a new series of ν_{CO} IR absorptions for $\text{Ru}_3(\text{CO})_9(\mu\text{-H})[(\mu_3, \eta^2\text{-P}(\text{C}_6\text{H}_5)_2(\text{C}_9\text{H}_7\text{N}))]_2$, **7**, that remained unchanged after 4 h of heating.



A single broad resonance at $\delta -11.2$ ppm and the absence of an indolyl NH resonance in the ^1H NMR spectrum suggested a net migration of a hydrogen atom to the triruthenium core.¹² An X-ray structure determination of **7**, a dark-red, air-stable solid was undertaken to determine the mode of ligand bonding and the position of the hydride in the cluster since the hydride resonance was too broad to exhibit ^{31}P -coupling.

Red needles of the cluster were grown from a solution of **7** in MeOH–hexanes (1 : 1) at -5°C over three weeks. Benzene- d_6 , used as a solvent during prior NMR analysis of this sample, co-crystallized with the cluster. An ORTEP representation is given in Fig. 4. Crystallographic data for the crystal $7\cdot\text{C}_6\text{D}_6$ is presented in Table 1 and a selection of bond distances and angles is given in Table 3. The triangular core of three ruthenium atoms is retained in the cluster. The ligand spans all three ruthenium atoms so as to cap one face of the triruthenium core. The P(1) atom, which was bound equatorially to Ru(1) in **4**, bonds axially to the Ru(1) atom of **7**. The Ru(1)–P(1) bond length of 2.377(1) Å is comparable to the Ru(1)–P(1) bond length of 2.3665(9) Å in **4**. The planar indolyl group effectively bisects the cluster in an orientation that is almost perpendicular (dihedral angle $88.9(1)^\circ$) to the triruthenium plane. Its N(1) atom is bonded axially and symmetrically to both Ru(2) and Ru(3) atoms with bond lengths of 2.191(4) and 2.168(4) Å, respectively. The Ru(2)–N(1)–Ru(3) bond angle is $79.4(1)^\circ$. The bridging hydride ligand H(1Ru) was located spanning the Ru(2)–Ru(3) edge of the metal triangle, sitting *trans* to the $\mu_3, \eta^2\text{-P}(\text{C}_6\text{H}_5)_2(\text{C}_9\text{H}_7\text{N})$ ligand. The Ru(2)–H(1Ru)–Ru(3) plane lies $60(2)^\circ$ away from the plane of the triruthenium core; the Ru(2)–H(1Ru)–Ru(3) angle is $93(3)^\circ$. Nine carbonyl groups complete the ligand shell of the cluster.

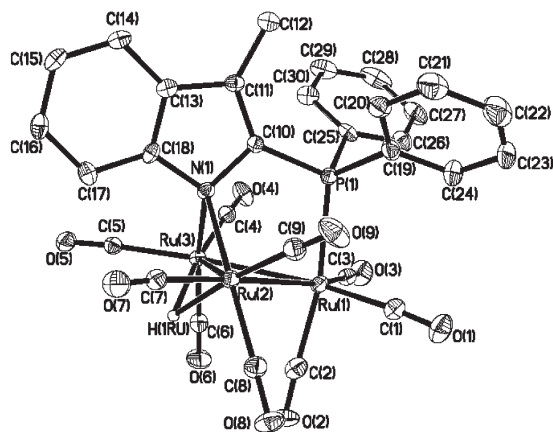


Fig. 4 ORTEP drawing of $\text{Ru}_3(\text{CO})_9(\mu\text{-H})[\mu_3, \eta^2\text{-P}(\text{C}_6\text{H}_5)_2(\text{C}_9\text{H}_7\text{N})]\cdot\text{C}_6\text{D}_6$ ($7\cdot\text{C}_6\text{D}_6$) with atoms shown as 30% probability ellipsoids. Phenyl hydrogen atoms and C_6D_6 have been omitted for clarity.

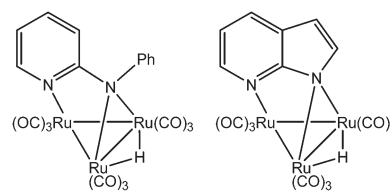
The solid-state structure of **7** most closely resembles that of $\text{Ru}_3(\text{CO})_9(\mu\text{-H})(\mu_3, \eta^2\text{-anpy})$ where anpy = 2-anilinopyridine and $\text{Ru}_3(\text{CO})_9(\mu\text{-H})(\mu_3, \eta^2\text{-ppy})$ where ppy = pyrrolo[2,3-*b*]pyridine.^{12,13} Both products were prepared by reactions of the ligands with $\text{Ru}_3(\text{CO})_{12}$ in refluxing hydrocarbon solvents. In neither case were intermediates or products with mono-coordinated ligands identified.

The anpy and ppy ligands adopt a similar geometry to that of **1** and, as anionic six-electron N,N-donors, bridge across the

Table 3 Selected bond distances (Å) and angles ($^\circ$) for cluster $7\cdot\text{C}_6\text{D}_6$

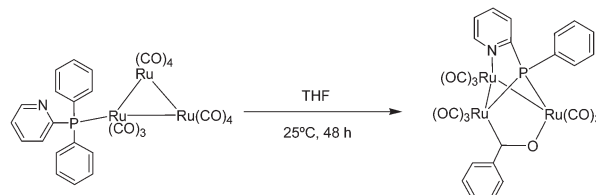
Ru(1)–Ru(2)	2.8026(7)	Ru(1)–Ru(2)–Ru(3)	60.31(2)
Ru(1)–Ru(3)	2.8068(7)	Ru(1)–Ru(3)–Ru(2)	60.16(2)
Ru(2)–Ru(3)	2.7848(7)	Ru(2)–Ru(1)–Ru(3)	59.53(2)
Ru(1)–P(1)	2.377(1)	Ru(1)–P(1)–C(10)	109.5(2)
Ru(2)–N(1)	2.191(4)	P(1)–C(10)–N(1)	114.5(3)
Ru(3)–N(1)	2.168(4)	C(10)–N(1)–C(18)	103.3(4)
N(1)–C(10)	1.446(6)	C(10)–N(1)–Ru(2)	117.3(3)
N(1)–C(18)	1.434(6)	C(10)–N(1)–Ru(3)	116.8(3)
P(1)–C(10)	1.797(5)	Ru(2)–N(1)–Ru(3)	79.4(1)
C(10)–C(11)	1.37(1)	Ru(3)–Ru(2)–N(1)	49.9(1)
C(11)–C(13)	1.451(7)	Ru(2)–Ru(3)–N(1)	50.7(1)
C(13)–C(18)	1.386(8)	C(10)–C(11)–C(13)	105.7(4)
Ru(2)–H(1Ru)	1.83(7)	C(11)–C(13)–C(18)	108.4(4)
Ru(3)–H(1Ru)	2.00(7)	C(13)–C(18)–N(1)	110.2(5)
		Ru(2)–H(1Ru)–Ru(3)	93(3)

triruthenium core to the remaining two ruthenium metals.^{12,13} In both instances, the hydride ligand is situated *trans* to the deprotonated nitrogen atom.



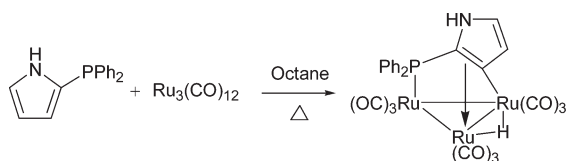
We propose that the indolyl substituent similarly acts as a four-electron donor in **7**. The N(1)–C(10) and N(1)–C(18) bonds of length 1.446(6) and 1.434(6) Å, respectively, are significantly longer than the corresponding bonds in **1** (1.399(2) and 1.373(2) Å), in **4** (1.389(4) and 1.380(4) Å), as well as when P-bound in the dimer $\text{Pd}_2\text{Cl}_4[\text{P}(\text{C}_6\text{H}_5)_2(\text{C}_9\text{H}_8\text{N})]_2$ (1.380(4) and 1.366(4) Å).¹ These bond lengths more closely resemble those of aromatic-C–four coordinate-N single bonds (average bond length = 1.465(7) Å)¹⁴ and are significantly longer than the analogous pyrrolo-pyridinate N–C bonds of $\text{Ru}_3(\text{CO})_9(\mu\text{-H})(\mu_3, \eta^2\text{-ppy})$ in which the disruption of ligand aromaticity is also reported.¹³ The nitrogen centre in **7** is therefore best considered as an sp^3 -hybridized centre which donates four electrons in a 48-electron cluster. The ability of **1** to behave as an anionic six-electron $\mu_3, \eta^2\text{-P,N}$ -donor polydentate ligand has been also observed in the formation of the novel cluster $\text{Pd}_4\text{Cl}_4[\text{P}(\text{C}_6\text{H}_5)_2(\text{C}_9\text{H}_8\text{N})]_2[\mu_3, \eta^2\text{-P}(\text{C}_6\text{H}_5)_2(\text{C}_9\text{H}_7\text{N})]_2$.¹⁵

Despite their common bonding features, the controlled metallation of **1** to cap the Ru_3 core is not observed in the subsequent reactions of the transient $\text{Ru}_3(\text{CO})_{11}\text{L}$ clusters of $\text{PPh}_2(2\text{-C}_4\text{H}_3\text{NH})$ and PPh_2Py . Rather, $\text{Ru}_3(\text{CO})_{11}(\text{PPh}_2\text{Py})$ spontaneously converts at room temperature into $\text{Ru}_3(\mu, \eta^2\text{-C}(\text{O})\text{Ph})[\mu_3, \eta^2\text{-P}(\text{Ph})(\text{C}_5\text{H}_4\text{N})](\text{CO})_9$ (Scheme 2)⁹ which features a bridging acyl group as a result of P–C bond cleavage. The cluster $\text{Ru}_3(\text{CO})_{11}[\text{Ph}_2\text{P}(2\text{-C}_4\text{H}_4\text{N})]$ was isolated in only small quantities as it readily loses carbonyl ligands to allow for metallation at the pyrrolyl ring to form $\text{Ru}_3(\text{CO})_9(\mu\text{-H})(\mu_3\text{-C}_4\text{H}_3\text{N})$ (Scheme 3).⁸ Notably, metallation of the pyrrolyl ring occurs at the C3 position, not at the nitrogen centre.



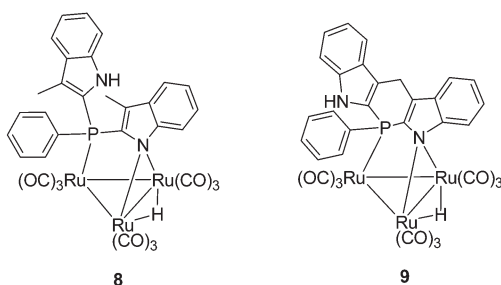
Scheme 2

The analogous clusters **8** and **9** were synthesized in a manner similar to **7** and exhibit comparable ν_{CO} IR absorption frequencies and relative intensities to **7**. The ^1H NMR spectra of **8** and **9** showed broad resonances at $\delta -11.2$ and -11.9 ppm, respec-



Scheme 3

tively, consistent with a hydride ligand bridging two ruthenium atoms in triruthenium clusters.¹² Broad NH resonances at δ 8.38 and 8.48 ppm, respectively, remain, indicating that indolyl metallation involves only one of the indolyl substituents while the other remains protonated. Based on the spectroscopic data, complexes **8** and **9** also represent 48-electron clusters with anionic six-electron $\mu_3, \eta^2\text{-P}(\text{C}_6\text{H}_5)(\text{C}_9\text{H}_8\text{N})(\text{C}_9\text{H}_7\text{N})$ and $\mu_3, \eta^2\text{-P}(\text{C}_6\text{H}_5)(\text{C}_{17}\text{H}_{11}\text{N}_2)$ bridging ligands, respectively.



Summary

The present study has demonstrated two coordination modes for indolylphosphine ligands. These ligands can serve as monodentate two-electron P-donors in substitution reactions with Ru₃(CO)₁₂. X-Ray structures of the Ru₃(CO)₁₁(HL) clusters confirm μ_1 and equatorial coordination of the phosphorus atom to the triruthenium core. Unlike the Ru₃ complexes of related P,N-donor ligands, gentle heating of the monosubstituted clusters is required to effect further reaction. This has permitted a degree of control over metallation of the indolyl moiety in capping the cluster to form Ru₃(CO)₉($\mu\text{-H}$)($\mu_3, \eta^2\text{-L}$) clusters without ligand fragmentation. The ligands in these compounds behave as novel and robust polydentate six-electron P,N-donors.

Experimental

General procedures

All reactions and manipulations were carried out under an atmosphere of nitrogen using standard Schlenk techniques unless otherwise stated. Ru₃(CO)₁₂ (Strem), sodium (ACP Chemicals) and benzophenone, dichloromethane, hexanes and methanol (Caledon) were used as received. Tetrahydrofuran was distilled from dark purple solutions of sodium benzophenone ketyl under a nitrogen atmosphere. Preparation of sodium benzophenone ketyl catalyst, ^{6b} P(C₆H₅)₂(C₉H₈N) (**1**),¹ P(C₆H₅)(C₉H₈N)₂ (**2**),¹ and P(C₆H₅)(C₁₇H₁₂N₂) (**3**)¹ were according to literature methods. All ¹H, ¹³C{¹H} and ³¹P{¹H} NMR were recorded on Varian XL 400 and Varian Mercury 300 spectrometers and referenced to 85% H₃PO₄ and SiMe₄ (TMS) in CDCl₃. IR spectra were recorded on a Nicolet 550 Magna FTIR spectrophotometer in absorbance mode. Elemental analyses were performed by ANALEST, Toronto, ON. X-Ray data were collected on a Nonius Kappa CCD diffractometer using graphite monochromated Mo-K α radiation ($\lambda = 0.71073 \text{ \AA}$). A combination of $1^\circ \phi$ and ω (with κ offsets) scans were used to collect sufficient data. The data frames were integrated and scaled using the Denzomn package. The structures were solved and refined with the SHELXTL-PC v5.1 software package. Refinement was by full-matrix least squares on F^2 using data (including negative intensi-

ties) with hydrogen atoms bonded to carbon atoms included in the calculated positions and treated as riding atoms.

CCDC reference numbers 243366–243369.

See <http://www.rsc.org/suppdata/dt/b4/b409930c/> for crystallographic data in CIF or other electronic format.

Ru₃(CO)₁₁[P(C₆H₅)₂(C₉H₈N)] 4. A mixture of Ru₃(CO)₁₂ (100 mg, 0.156 mmol) and **1** (30 mg, 0.159 mmol) in anhydrous tetrahydrofuran (12 mL) was heated to 40 °C to dissolve the cluster. A sodium benzophenone ketyl solution (five drops) was added dropwise *via* syringe until the solution became dark red. The reaction was monitored by IR spectroscopy until completion. After 15 min, the solvent was removed *in vacuo*, leaving a red residue. The product was separated by column chromatography with an eluent of hexanes–dichloromethane (3:1). The first orange band was found to be Ru₃(CO)₁₂ while the second red band was found to be the product. Removal of the solvent from the second band gave a red solid (123 mg, 85%). Red plates suitable for a single-crystal X-ray diffraction study were grown by evaporation of a saturated hexanes solution of the cluster at room temperature over 8 h. ³¹P{¹H} NMR (CD₂Cl₂): δ 15.9 (s). ¹H NMR (CD₂Cl₂): δ 8.34 (br s, 1H, NH), 7.21–7.71 (m, 14H) and 1.95 (s, 3H, CH₃ on indole). ¹³C{¹H} NMR (CD₂Cl₂): δ 204.2 (br s, CO), 137.2 (d, C8, ⁴J_{CP} = 8 Hz), 133.8 (d, Ph–C_{is}, ¹J_{CP} = 47 Hz), 132.2 (d, Ph–C_o, ²J_{CP} = 12 Hz), 130.8 (d, Ph–C_p, ⁴J_{CP} = 2 Hz), 130.0 (d, C9, ³J_{CP} = 8 Hz), 129.0 (d, Ph–C_m, ³J_{CP} = 11 Hz), 124.3 (s, C6), 123.5 (d, C3, ³J_{CP} = 60 Hz), 120.6 (d, C2, ¹J_{CP} = 8 Hz), 120.2 (s, C5), 119.5 (s, C4), 111.4 (s, C7) and 10.7 (s, CH₃ on indole). IR (ν_{CO} , cm⁻¹, CH₂Cl₂): 2099 (m), 2048 (s) and 2014 (m). Anal. Calc. for C₃₂H₁₈NO₁₁PRu₃: C, 41.48; H, 1.96; N, 1.51. Found: C, 41.62; H, 2.01; N, 1.39%.

Ru₃(CO)₁₁[P(C₆H₅)(C₉H₈N)] 5. In anhydrous tetrahydrofuran (12 mL), a solution of Ru₃(CO)₁₂ (110 mg, 0.172 mmol) and **2** (60 mg, 0.163 mmol) was heated to 40 °C to dissolve the cluster. The product was prepared in the same manner as **4** to give a red solid (139 mg, 87%). Red plates suitable for a single-crystal X-ray diffraction study were grown by evaporation of a saturated hexanes solution of the cluster at room temperature over 10 h. ³¹P{¹H} NMR (CD₂Cl₂): δ -1.48 (s). ¹H NMR (CD₂Cl₂): δ 8.26 (br s, 2H, NH), 7.00–7.75 (m, 13H) and 2.08 (s, 6H, CH₃ on indole). ¹³C{¹H} NMR (CD₂Cl₂): δ 203.9 (br s, CO), 137.2 (d, C8, ⁴J_{CP} = 8 Hz), 133.2 (d, Ph–C_{is}, ¹J_{CP} = 50 Hz), 131.6 (d, Ph–C_o, ²J_{CP} = 12 Hz), 130.9 (s, Ph–C_p), 130.0 (d, C9, ³J_{CP} = 8 Hz), 129.2 (d, Ph–C_m, ³J_{CP} = 11 Hz), 124.4 (s, C6), 121.9 (d, C3, ³J_{CP} = 62 Hz), 120.5 (d, C2, ¹J_{CP} = 8 Hz), 120.3 (s, C5), 119.5 (s, C4), 111.6 (s, C7) and 10.3 (s, CH₃ on indole). IR (ν_{CO} , cm⁻¹, CH₂Cl₂): 2100 (m), 2050 (s) and 2017 (m). Anal. Calc. for C₃₅H₂₁N₂O₁₁PRu₃: C, 42.91; H, 2.16; N, 2.86. Found: C, 42.89; H, 2.17; N, 2.75%.

Ru₃(CO)₁₁[P(C₆H₅)(C₁₇H₁₂N₂)] 6. A solution of Ru₃(CO)₁₂ (96 mg, 0.150 mmol) and **3** (50 mg, 0.142 mmol) in anhydrous tetrahydrofuran (12 mL) was heated to 40 °C to dissolve the cluster. The product was prepared in the same manner as **4** to give a red solid (112 mg, 82%). Red needles suitable for a single-crystal X-ray diffraction study were grown by evaporation of a saturated hexanes solution of the cluster at room temperature over 6 h. ³¹P{¹H} NMR (CD₂Cl₂): δ -13.9 (s). ¹H NMR (CD₂Cl₂): δ 8.28 (br s, 2H, NH), 7.10–7.93 (m, 13H), 4.54 (dd, 1H, CH₂ bridge, ²J_{HH} = 21 Hz, ⁴J_{HP} = 5 Hz) and 4.42 (dd, 1H, CH₂ bridge, ²J_{HH} = 21 Hz, ⁴J_{HP} = 5 Hz). ¹³C{¹H} NMR (CD₂Cl₂): δ 204.0 (br s, CO), 139.33 (d, C8, ³J_{CP} = 8 Hz), 133.8 (d, Ph–C_{is}, ¹J_{CP} = 43 Hz), 132.3 (d, Ph–C_o, ²J_{CP} = 14 Hz), 131.6 (d, Ph–C_p, ⁴J_{CP} = 3 Hz), 129.3 (d, Ph–C_m, ³J_{CP} = 11 Hz), 126.4 (d, C9, ³J_{CP} = 7 Hz), 126.2 (d, C2, ¹J_{CP} = 17 Hz), 124.3 (s, C6), 120.6 (s, C4), 119.6 (s, C5), 122.0 (d, C3, ²J_{CP} = 5 Hz), 111.7 (s, C7) and 20.9 (s, CH₂ bridge). IR (ν_{CO} , cm⁻¹, CH₂Cl₂): 2097 (m), 2048 (s) and 2014 (m). Anal. Calc. for C₃₄H₁₇N₂O₁₁PRu₃: C, 42.38; H, 1.78; N, 2.91. Found: C, 42.04; H, 1.84; N, 3.19%.

Ru₃(CO)₉(μ-H)[μ₃,η²-P(C₆H₅)₂(C₉H₇N)] 7. When **4** (50 mg, 0.054 mmol) was heated at 70 °C in hexane (10 mL), a dark brown solution formed. Monitoring by IR spectroscopy in the ν_{CO} region revealed complex formation with 100% spectroscopic yields within 4 h. The solvent was then removed *in vacuo*, leaving a brown residue. The product (first band) was separated by column chromatography with an eluent of hexanes–acetone (4 : 1), giving a brown–red solid. The powder was recrystallized from methanol–hexanes (1 : 1) at –5 °C over 3 weeks to give red needles suitable for a single-crystal X-ray diffraction study (24 mg, 52%). ³¹P{¹H} NMR (CD₂Cl₂): δ 21.6 (s). ¹H NMR (CD₂Cl₂): δ 7.02–7.87 (m, 14H), 2.20 (s, 3H, CH₃ on indole) and –11.1 (s, Ru–H). IR (ν_{CO}, cm^{–1}, CH₂Cl₂): 2083 (m), 2057 (s), 2028 (s) and 2003 (m). Anal. Calc. for C₃₀H₁₈NO₉PRu₃: C, 41.39; H, 2.08; N, 1.61. Found: C, 41.70; H, 2.06; N, 1.54%.

Ru₃(CO)₉(μ-H)[μ₃,η²-P(C₆H₅)(C₉H₇N)(C₉H₇N)] 8. **5** (50 mg, 0.051 mmol) was heated at 75 °C in hexane (10 mL), forming a dark brown solution. The reaction was monitored by IR spectroscopy in the ν_{CO} region for 4 h. The solvent was then removed *in vacuo*, leaving a tan brown residue. The product (third band) was separated by column chromatography with an eluent of hexanes–dichloromethane (1 : 1), giving a red–brown solid (23 mg, 49%). ³¹P{¹H} NMR (benzene-d₆): δ 1.82 (s). ¹H NMR (benzene-d₆): δ 8.38 (s, 1H, NH) 7.09–7.74 (m, 13H), 1.82 (s, 3H, CH₃ on indole) and –11.2 (s, Ru–H). IR (ν_{CO}, cm^{–1}, CH₂Cl₂): 2070 (m), 2045 (s), 2020 (s) and 1992 (m). Anal. Calc. for C₃₃H₂₁N₂O₉PRu₃: C, 42.91; H, 2.29; N, 3.03. Found: C, 42.61; H, 2.23; N, 2.75%.

Ru₃(CO)₉(μ-H)[μ₃,η²-P(C₆H₅)(C₁₇H₁₁N₂)] 9. A brown solution formed when **6** (50 mg, 0.052 mmol) was heated at 75 °C in hexane (10 mL). The reaction was monitored by IR spectroscopy in the ν_{CO} region for 5 h. The solvent was then removed *in vacuo*, leaving a purple–brown residue. The product was separated by column chromatography as the fourth band with an eluent of hexanes–acetone (4 : 1) and further purified with an eluent of hexanes–dichloromethane (1 : 1) as the first band, giving a purple–brown solid (22 mg, 46%). ³¹P{¹H} NMR (benzene-d₆): δ –11.9 (s). ¹H NMR (benzene-d₆): δ 8.43 (s, 1H, NH), 7.05–7.47 (m, 13H), 4.59 (dd, 1H, CH₂ bridge, ²J_{HH} = 22 Hz, ⁴J_{HP} = 5 Hz), 4.47 (dd, 1H, CH₂ bridge, ²J_{HH} = 22 Hz, ⁴J_{HP} = 5 Hz) and –11.9 (s, Ru–H). IR (ν_{CO}, cm^{–1}, CH₂Cl₂): 2081 (m), 2050 (s), 2030 (s) and 2007 (m). Anal. Calc. for

C₃₂H₁₇N₂O₉PRu₃: C, 42.34; H, 1.89; N, 3.09. Found: C, 42.38; H, 1.79; N, 2.90%.

Acknowledgements

We thank Mr Dan Mathers for performing elemental analyses. The study was supported by the University of Toronto Open Fellowship.

References

- 1 J. O. Yu, E. Lam, J. C. Sereda, N. Rampersad, D. H. Farrar, C. Scott Browning and A. J. Lough, *Organometallics*, accepted, (OM0401004).
- 2 A. R. Katritzky, P. Lue and Y. Chen, *J. Org. Chem.*, 1990, **55**, 3688–3691.
- 3 (a) J. P. Farr, F. E. Wood and A. L. Balch, *Inorg. Chem.*, 1983, **22**, 3387–3393; (b) N. Lugan, G. Lavigne, J. Bonnet, R. Réau, D. Neibecker and I. Tkatchenko, *J. Am. Chem. Soc.*, 1988, **110**, 5369–5376; (c) E. Rotondo, S. L. Schiavo, G. Bruno, C. G. Arena, R. Gobetto and F. Faraone, *Inorg. Chem.*, 1989, **28**, 2944–2949; (d) T. Suzuki and J. Fujita, *Chem. Lett.*, 1992, 1067–1068.
- 4 U. Berens, J. M. Brown, J. Long and R. Selke, *Tetrahedron: Asymmetry*, 1996, **7**, 285–292.
- 5 A. J. Deeming and M. K. Shinmar, *J. Organomet. Chem.*, 1999, **592**, 235–239.
- 6 (a) M. I. Bruce, D. C. Kehoe, J. G. Matison, B. K. Nicholson, P. H. Rieger and M. L. Williams, *Chem. Commun.*, 1982, 442–444; (b) M. I. Bruce, J. G. Matison and B. K. Nicholson, *J. Organomet. Chem.*, 1983, **247**, 321–343; (c) C. J. Adams, M. I. Bruce, P. A. Duckworth, P. A. Humphrey, O. Kuhl, E. R. T. Tiekink, W. R. Cullen, P. Braunstein, S. C. Cea, B. W. Skelton and A. H. White, *J. Organomet. Chem.*, 1994, **467**, 251–181.
- 7 E. J. Forbes, N. Goodhand, D. L. Jones and T. A. Hamor, *J. Organomet. Chem.*, 1979, **182**, 143–154.
- 8 A. J. Arce, A. J. Deeming, Y. De Sanctis, S. K. Johal, C. M. Martin, M. Shinmar, D. M. Speel and A. Vassos, *Chem. Commun.*, 1998, 233–234.
- 9 N. Lugan, G. Lavigne and J.-J. Bonnet, *Inorg. Chem.*, 1987, **26**, 585–590.
- 10 A. J. Deeming, S. E. Kabir, N. I. Powell, P. A. Bates and M. B. Hursthouse, *J. Chem. Soc., Dalton Trans.*, 1987, 1529–1534.
- 11 M. I. Bruce, P. A. Humphrey, O. Shawkataly, M. R. Snow, E. R. T. Tiekink and W. R. Cullen, *Organometallics*, 1990, **9**, 2910–2919.
- 12 P. L. Andreu, J. A. Cabeza, V. Riera, Y. Jeannin and D. Miguel, *J. Chem. Soc., Dalton Trans.*, 1990, 2201–2206.
- 13 J. A. Cabeza, L. A. Oro, A. Tiripicchio and M. Tiripicchio-Camellini, *J. Chem. Soc., Dalton Trans.*, 1988, 1437–1444.
- 14 F. H. Allen, O. Kennard, D. G. Watson, L. Brammer, A. G. Orpen and R. Taylor, *J. Chem. Soc., Perkin Trans. 2*, 1987, S1–S19.
- 15 E. Lam, J. O. Yu, D. H. Farrar, C. Scott Browning and A. J. Lough, unpublished.